The Journal of Neuroscience, July 1, 2000, 20(13):4769–4775

Alternative Splicing in the Cytoplasmic II–III Loop of the N-Type Ca Channel α_{1B} Subunit: Functional Differences Are β Subunit-Specific

Jennifer Qian Pan and Diane Lipscombe

Department of Neuroscience, Brown University, Providence, Rhode Island 02912

Structural diversity of voltage-gated Ca channels underlies much of the functional diversity in Ca signaling in neurons. Alternative splicing is an important mechanism for generating structural variants within a single gene family. In this paper, we show the expression pattern of an alternatively spliced 21 amino acid encoding exon in the II–III cytoplasmic loop region of the N-type Ca channel α_{1B} subunit and assess its functional impact. Exon-containing α_{1B} mRNA dominated in sympathetic ganglia and was present in ~50% of α_{1B} mRNA in spinal cord and caudal regions of the brain and in the minority of α_{1B} mRNA in neocortex, hippocampus, and cerebellum (<20%). The II–III loop exon affected voltage-dependent inactivation of the N-type Ca channel. Steady-state inactivation curves were shifted to more depolarized potentials without affects on either the rate or voltage dependence of channel opening. Differences in voltage-dependent inactivation between α_{1B} splice variants were most clearly manifested in the presence of Ca channel β_{1b} or β_4, rather than β_{2a} or β_3, subunits. Our results suggest that exon-lacking α_{1B} splice variants that associate with β_{1b} and β_4 subunits will be susceptible to voltage-dependent inactivation at voltages in the range of neuronal resting membrane potentials (−60 to −80 mV). In contrast, α_{1B} splice variants that associate with either β_{2a} or β_3 subunits will be relatively resistant to inactivation at these voltages. The potential to mix and match multiple α_{1B} splice variants and β subunits probably represents a mechanism for controlling the plasticity of excitation–secretion coupling at different synapses.

Key words: N-type calcium channel; α_1 subunit; regulated alternative splicing; intracellular loop II–III; genomic analysis; tissue distribution; β subunit

Structural diversity of voltage-gated Ca channels is at the heart of the rich functional diversity in Ca signaling in mammalian neurons. Neurons can select from several distinct Ca channel α_1 genes that undergo extensive RNA processing, including alternative splicing (Perez-Reyes et al., 1990; Soldatov, 1994; Kollmar et al., 1997; Lin et al., 1997; Bourinet et al., 1999) and differential polyadenylation (Schorge et al., 1999). Each α_1 subunit may also interact with multiple functionally distinct auxiliary subunits (Scott et al., 1996; Walker and De Waard, 1998), expanding the capacity for diversity within each Ca channel family. The α_{1B} subunit is the functional core of N-type Ca channels that localize to synapses and control calcium-dependent neurotransmitter release throughout the vertebrate nervous system (Hirning et al., 1988; Takahashi and Momiyama, 1993; Dunlap et al., 1995). Many neurotransmitters and neurohormones modulate excitation–secretion coupling by regulating the gating of N-type Ca channels via effects on the α_{1B} subunit (Dunlap et al., 1995). The α_{1B} gene is also subject to tissue-specific alternative splicing (Lin et al., 1997, 1999), which probably represents an important mechanism for optimizing neurotransmitter release in different regions of the nervous system. The extent of splicing in the α_{1B} gene is not known, but its large size (>100 kb in human genome), together with mismatches in α_{1B} cDNAs isolated from different tissues, supports the presence of multiple sites of alternative splicing.

In a previous study, we identified two short cassette exons in S3–S4 linkers of domains III and IV of the Ca channel α_{1B} subunit gene (see Fig. 1*A*) (Lin et al., 1997, 1999). Alternative splicing of these exons was tissue-specific and influenced both the voltage-dependence and rate of Ca channel activation. A third variant site in loop I–II of the of α_{1B} gene involving one amino acid (A^{415}) originated from the random use of alternative 3′ acceptor–splice sites, but it is not associated with any obvious change in channel gating (Lin et al., 1997). In the present study, we characterize a larger alternatively spliced sequence encoding 21 amino acids in the cytoplasmic II–III loop of the α_{1B} gene (see Fig. 1*A*) first identified in mouse neuroblastoma cells (Coppola et al., 1994) and more recently shown by PCR analysis to be present in rat brain (Ghasemzadeh et al., 1999). We report the genomic structure of this site in the rat α_{1B} gene, detail the differential expression of this exon in the rat nervous system, and assess its impact on channel function.

MATERIALS AND METHODS

Genomic analysis. A 6.3 kb region of the rat α_{1B} gene was amplified from liver genomic DNA using primers directed to 5′ and 3′ exons flanking the splice junction of interest in the II–III loop region. Primer sequences were as follows: Bup2170, (5′-GAG GAG ATG GAA GAG GCA GCC AAT-3′); and Bdw2361, (5′-CTC CGG GTC CAT CTC ACT GTA CAG T-3′). The 50 μl PCR reaction mix contained 250 ng of rat liver genomic DNA, 350 μM each deoxynucleotide and 0.4 μM each primer. After a 15 min preincubation at 92°C, 0.75 μl of enzyme mix (Expand Long Template; Boehringer Mannheim, Indianapolis, IN) was added to "hot start" the reaction. After 30 amplification cycles, a single 6.3 kb product was generated and subsequently gel-purified, subcloned, and sequenced by primer walking (Yale University Sequencing Facility, New Haven, CT). The sequence is available under GenBank accession number AF222338.

Received Feb. 11, 2000; revised April 4, 2000; accepted April 11, 2000.

This work was supported by National Institutes of Health Grants NS29967 and NS01927 (D.L.). We are grateful to Kevin Campbell for β_{1b} cDNA and Edward Perez-Reyes for β_{2a} and β_4 cDNAs. Julie Nam assisted in some of the PCR experiments. We thank members of the Lipscombe laboratory and Dr. Yael Amitai for comments on this manuscript.

Correspondence should be addressed to Diane Lipscombe, Department of Neuroscience, 192 Thayer Street, Brown University, Providence, RI 02912. E-mail: diane_lipscombe@brown.edu.

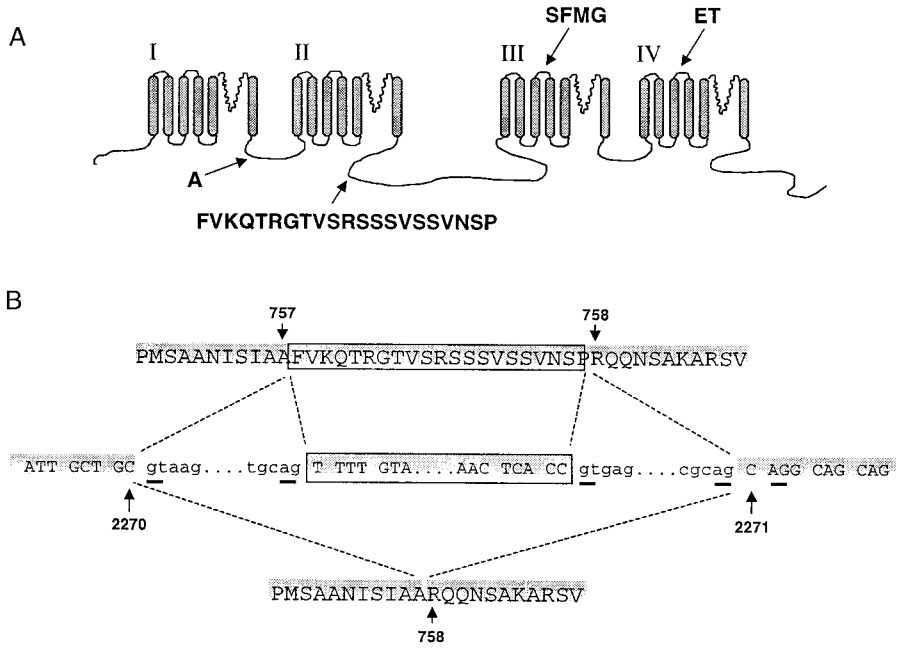

Figure 1. Sites of alternative splicing in the N-type calcium channel α_{1B} subunit. *A*, Putative membrane topology of the α_{1B} subunit and location of four alternatively spliced sequences encoding Ala^{415} in intracellular loop I–II (*A*), 21 amino acids in intracellular loop II–III (*FVKQTRGTVSRSSSVSSVNSP*), four amino acids in IIIS3–IIIS4 (*SFMG*), and two amino acids in IVS3–IVS4 (*ET*). With the exception of Ala^{415} whose expression depends on the use of alternative 3′ splice–acceptors, expression of the other three sites is regulated by alternative splicing of isolated exon cassettes (Lin et al., 1997, 1999). *B*, Genomic sequence derived from analysis of the α_{1B} gene in the region of the intracellular II–III loop (*middle*) together with the amino acid sequences of two cDNAs derived by RT-PCR from rat neurons (*top*, *bottom*). The location of exons (*uppercase letters*, *shaded*), introns (*lowercase*), the 63 base exon cassette (*boxed*), and splice junction consensus *ag-gt* dinucleotide sequences (*underlined*) are indicated. Nucleotides *2270* and *2271* and amino acids A^{757} (*757*) and R^{758} (*758*) denote the splice junction (numbering according to GenBank sequence M92905) (Dubel et al., 1992). *Dashed lines* indicate the two patterns of alternative splicing that give rise to $+21\alpha_{1B}$ (*top*) and $\Delta21\alpha_{1B}$ (*bottom*). The genomic sequence of this region is available under GenBank accession number AF222338.

Reverse transcription-PCR. Total RNA was isolated from different regions of the adult rat nervous system using the guanidium–thiocyanate method and used for first strand cDNA synthesis; 4–6 μg of RNA from CNS tissue or 1–2 μg of RNA from sensory and sympathetic ganglia was used as template in each 20 μl reaction mix containing 0.5 mM each deoxynucleotide, 50 ng/μl random hexamers, 10 mM DTT, and 200 U Moloney murine leukemia virus reverse transcriptase (Life Technologies, Grand Island, NY), incubated for 1 hr at 37°C. One microliter of cDNA from each reverse transcription (RT) reaction (or 3 μl from pituitary RT reaction) was used for PCR amplification in a 50 μl standard reaction mix using the following protocol: 1 cycle at 94°C for 2 min, 30 cycles at 94°C for 10 sec, 59°C for 35 sec, 72°C for 50 sec, and 1 cycle at 72°C for 8 min. Primers Bup2104 (5′-TTG AAC GTT TTC TTG GCC ATT GCT GT) and Bdw2363 (5′- CTC CTC CGG GTC CAT CTC ACT GTA CA) were located in 5′ and 3′ exons flanking the splice junction. Negative controls that lacked template confirmed that reagents were not contaminated by α_{1B} cDNA clones. The primers flanked a 6.1 kb intron so contamination by genomic DNA could be ruled out, and reverse transcriptase-lacking controls were also performed. Thirty rounds of amplification were used routinely in our analysis. To control for the possibility of saturation, the number of cycles was increased stepwise from 10, 15, 20, 25, to 30 in one experiment. Products were first observed after 25 cycles, and relative band intensities were identical to those observed after 30 cycles. Band intensities were quantified and normalized to the size of the DNA fragments using a gel documentation system (Alpha Inotech).

Functional assessment of the Ca channel α_{1B} cDNA constructs. The N-type Ca channel $\alpha_{1B\text{-}b}$ splice variant (Lin et al., 1997) (GenBank accession number AF055477) referred to here as $\Delta21\alpha_{1B}$ was used as template for constructing the $+21\alpha_{1B}$ splice variant (GenBank accession number AF222337) by standard cloning methods. $\Delta21\alpha_{1B}$ and $+21\alpha_{1B}$ splice variants were cloned into the *Xenopus* β-globin vector pBSTA to facilitate functional expression (Goldin and Sumikawa, 1992). Functional properties of $\Delta21\alpha_{1B}$ and $+21\alpha_{1B}$ were assessed in the *Xenopus* oocyte expression system using methods and procedures essentially as described previously (Lin et al., 1997, 1999). Forty-six nanoliters of α_{1B} (67–400 ng/μl) and β (22–133 ng/μl) cRNA mix (α_{1B}/β is 3:1 μg/μg) were injected into defolliculated *Xenopus* oocytes, and currents were recorded 3–5 d later. Before recording, oocytes were injected with 46 nl of a 50 mM BAPTA solution to reduce activation of the endogenous Ca-activated Cl^- current (Lin et al., 1997). N-type Ca^{2+} channel currents were recorded with the two microelectrode voltage-clamp technique using electrodes of 0.8–1.5 and 0.3–0.5 MΩ resistance (3 M KCl) for voltage and current electrodes, respectively. Recording solutions contained either 5 mM $BaCl_2$ or 2 mM $CaCl_2$, 85 mM tetraethylammonium, 5 mM KCl, and 5 mM HEPES, pH adjusted to 7.4 with methanesulfonic acid. The β_{1b} subunit used in this study was provided by K. P. Campbell (University of Iowa, Iowa City, IA) (Pragnell et al., 1992); β_{2a} and β_4 was provided by E. Perez-Reyes (Loyola University, Maywood, IL) (Perez-Reyes et al., 1992; Castellano et al., 1993b), and β_3 was cloned in our lab from rat brain and is almost identical to the published rat brain sequence (Castellano et al., 1993a). Both Ca channel α_{1B} splice variants expressed equally well in *Xenopus* oocytes [e.g., in the presence of β_3, the average N channel current amplitude was 2.68 ± 0.26 μA ($n = 8$) compared with 2.46 ± 0.11 μA ($n = 7$) for $+21\alpha_{1B}$ and $\Delta21\alpha_{1B}$, respectively]. With the exception of β_4, Ca currents were twofold to threefold larger in oocytes expressing α_{1B} together with a β subunit. β_4 did not increase current amplitude, but it did modulate N channel gating, confirming that it was expressed (see Results). Data were acquired on-line and leak subtracted using a P/4 protocol (pClamp V6.0; Axon Instruments, Foster City, CA). Voltage steps were applied every 10–30 sec depending on the duration of the step, from various holding potentials. Current-voltage and steady-state inactivation relationships and activation and inactivation rates were measured.

RESULTS

We analyzed the α_{1B} gene to determine whether alternative splicing could explain the presence of α_{1B} cDNA variants containing an extra 21 amino acid encoding sequence in the II–III intracellular loop region. The salient features of this region of the α_{1B} gene are presented in Figure 1*B*. A single 6.3 kb product was amplified from rat genomic DNA using PCR primers directed to cDNA sequences flanking the putative alternatively spliced exon. We sequenced this product and showed that codon A757 is interrupted by a 6125 bp intronic sequence that contains consensus *gt* and *ag* splice junctions (Sharp and Burge, 1997). A 63 base cassette exon was identified midway through the intronic sequence flanked by *ag-gt* splice junction motifs (Fig. 1*B*) and a polypyrimidine track 5′ to the exon (data not shown). The sequence of the cassette exon corresponds to the 63 base insert, confirming that $+21\alpha_{1B}$ and $\Delta21\alpha_{1B}$ variants that we (Fig. 2) (Pan et al., 1999) and others have observed in the II–III loop region of α_{1B} mRNA (Coppola et al., 1994; Ghasemzadeh et al., 1999) arise from alternative splicing. In their study, Coppola et al. (1994) showed that the alternatively expressed sequence contained 66, rather than 63, bases. This is because all α_{1B} cDNAs isolated from mouse neuroblastoma cells that lacked the 63 base

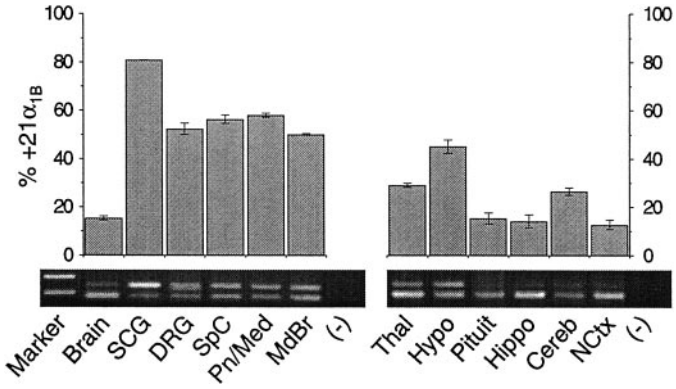

Figure 2. Expression pattern of $+21\alpha_{1B}$ and $\Delta21\alpha_{1B}$ mRNAs in various regions of the nervous system of the adult rat. *Top*, Summary of RT-PCR analysis showing the relative abundance of the $+21\alpha_{1B}$ mRNA variant expressed as a fraction of total α_{1B} mRNA derived from brain (*Brain*), superior cervical ganglia (*SCG*), dorsal root ganglia (*DRG*), spinal cord (*SpC*), pons and medulla (*Pn/Med*), midbrain (*MdBr*), thalamus (*Thal*), hypothalamus (*Hypo*), pituitary (*Pituit*), hippocampus (*Hippo*), cerebellum (*Cereb*), neocortex (*NCtx*), and template negative PCR controls (−). Data were averaged from analysis of at least three different RNA samples for each tissue isolated from multiple rats (mean ± SE). *Bottom*, Example of PCR-derived cDNAs separated by electrophoresis in 2% agarose. Two cDNA products were amplified from each sample (285 and 348 bp) corresponding to $\Delta21\alpha_{1B}$ and $+21\alpha_{1B}$ mRNA. The *first lane* shows 300 and 400 bp size markers. One microliter of RT reaction, except for pituitary (3 μl), was used as template for PCR amplification for all RNA samples. Relative band intensities were estimated using Alpha Inotech gel documentation software and normalized for size differences.

exon sequence also lacked three bases encoding R758. Figure 1*B* shows that the R758 codon is not part of the isolated 63 base exon but rather is contiguous with the 3′ flanking exon, and its expression depends on the use of alternative dinucleotide, *ag*, splice–acceptors at this distal 3′ intron–exon boundary (flanking nucleotide 2271) (Fig. 1*B*). Use of the first splice–acceptor site would result in α_{1B} mRNA containing the R758 codon, whereas R758 would be skipped if the second splice–acceptor site is used. All α_{1B} clones that we have so far isolated from rat contain R758, but the presence of R758-lacking α_{1B} clones in mouse neuroblastoma cells (Coppola et al., 1994) and bovine chromaffin cells (Cahill et al., 2000) confirms that both splice–acceptor sites are used. We have not investigated the expression pattern or the functional consequences of R758 but rather focused on the 63 base cassette exon.

To determine the expression pattern of the 63 base cassette exon, we analyzed RNA isolated from different regions of the nervous system of the adult rat by RT-PCR (Fig. 2). PCR primers that flanked the splice junction were chosen to generate two readily separable size cDNA products (348 and 285 bp) corresponding to $+21\alpha_{1B}$ and $\Delta21\alpha_{1B}$ mRNAs, respectively. Contamination by genomic DNA could be excluded because the primers flanked a 6.1 kb intron. By measuring relative band intensities, we show that exon expression is differentially regulated in different regions of the nervous system. $+21\alpha_{1B}$ mRNA dominates in sympathetic ganglia (80.8 ± 0.2% of total α_{1B}, $n = 3$), whereas exon expression is suppressed in α_{1B} mRNA isolated from whole brain (15.3 ± 0.8% of total α_{1B}, $n = 3$). Exon expression was not, however, suppressed uniformly throughout the CNS. Although relatively low levels of $+21\alpha_{1B}$ mRNA (<20% total α_{1B}) were present in neocortex, hippocampus, and pituitary, reflecting the pattern in whole brain, significant amounts of both splice variants ($+21\alpha_{1B}$ and $\Delta21\alpha_{1B}$) were detected in more caudal regions of the CNS, including spinal cord and brainstem.

Having established that alternative splicing in the II–III intracellular loop region of α_{1B} is strongly region-specific, we next determined whether exon expression affected channel function. The kinetics and voltage dependence of N-type Ca channel activation and inactivation were studied in oocytes expressing $\Delta21\alpha_{1B}$ and $+21\alpha_{1B}$ splice variants. At least three different β subunits copurify with α_{1B} in native membranes (Scott et al., 1996), and heterologous expression studies have shown that multiple β subunits modulate N-type Ca channel function (Walker and De Waard, 1998). We therefore thought it pertinent to assess the functional impact of splicing in the presence of four different Ca channel β subunits known to be expressed in rat brain (β_{1b}, β_{2a}, β_3, and β_4) (Pragnell et al., 1991; Perez-Reyes et al., 1992; Castellano et al., 1993a,b).

Figure 3 compares N-type currents induced by expressing $\Delta21\alpha_{1B}$ and $+21\alpha_{1B}$ splice variants in *Xenopus* oocytes in the presence of each β subunit. $\Delta21\alpha_{1B}$ and $+21\alpha_{1B}$ splice variants expressed equally well in oocytes, and their normalized, peak current–voltage curves and channel activation kinetics were indistinguishable. Peak current–voltage curves for Ca channels recorded from oocytes expressing β_3 were shifted by ~10 mV in the depolarizing direction relative to β_{1b}, β_{2a}, and β_4 similarly for both α_{1B} splice variants (see also Fig. 5*A*). We therefore conclude that the presence of an additional 21 amino acids in the cytoplasmic II–III loop of the α_{1B} subunit does not affect the kinetics or voltage dependence of N-type Ca channel opening.

N-type Ca channels recorded from native cells vary considerably in their voltage dependence and kinetics of inactivation (Bean, 1989). We therefore compared both the time course of inactivation and steady-state inactivation curves of $\Delta21\alpha_{1B}$ and $+21\alpha_{1B}$ splice variants in the presence of different β subunits. Normalized, averaged currents recorded from oocytes expressing each α_{1B}/β combination are shown as *insets* in Figure 4*A–D*. Inactivation kinetics of the splice variants are indistinguishable in the presence of a given β subunit, and superimposed averaged currents overlap almost perfectly. The kinetics of N-type Ca channel inactivation did, however, vary depending on the type of β subunit expressed. For example, N-type Ca channel currents recorded in β_{1b}- and β_3-expressing oocytes inactivate with relatively fast time courses compared with β_{2a} similarly for both α_{1B} splice variants (Fig. 4). These findings are consistent with other studies that associate the presence of β_{2a} with relatively slowly inactivating Ca channels (Olcese et al., 1994; Walker and De Waard, 1998). Alternative splicing in the II–III loop of the α_{1B} subunit does not, therefore, affect channel inactivation kinetics during step depolarizations to relatively positive voltages. However, a significant difference in the N-type Ca channel availability curve was observed between $\Delta21\alpha_{1B}$ and $+21\alpha_{1B}$ when the holding potential was varied. N-type Ca channels induced by expressing $+21\alpha_{1B}$ splice variant with β_{1b} and β_4 inactivated at membrane potentials that were ~10 mV more depolarized relative to $\Delta21\alpha_{1B}$ (Fig. 4*A*,*D*; see also Fig. 6*B*). These differences were only revealed in the presence of specific α_{1B}/β subunit combinations because steady-state inactivation curves were similar between α_{1B} splice variants when coexpressed with β_{2a} and only slightly different in the presence of β_3 (Fig. 4*B*,*C*; see also Fig. 6*B*).

In Figure 5 we compare normalized current–voltage and steady-state inactivation curves of the four different β subunits expressed with one α_{1B} splice variant ($\Delta21\alpha_{1B}$). With the exception of β_3, which is associated with Ca channel currents activating

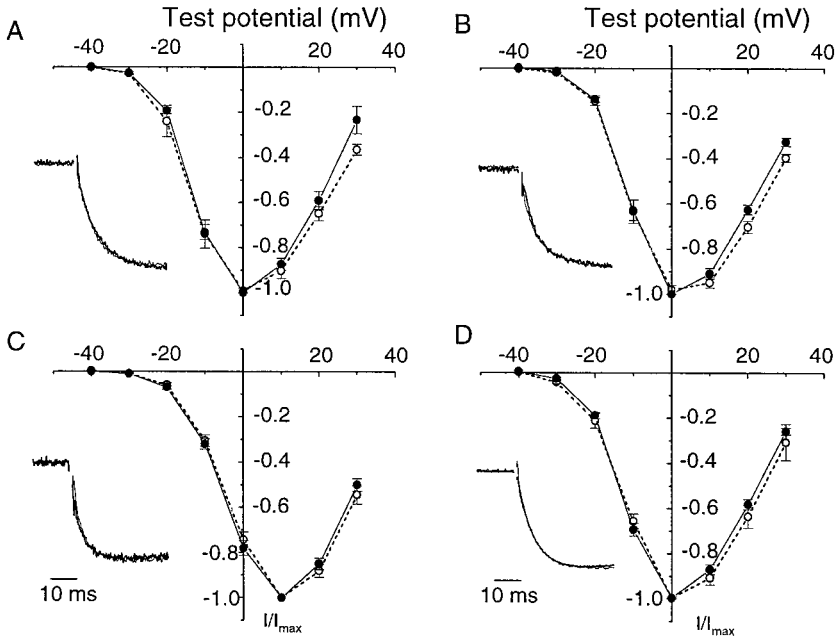

Figure 3. $+21\alpha_{1B}$ and $\Delta21\alpha_{1B}$ splice variants have similar voltage- and time-dependent activation properties. Normalized, averaged peak current–voltage plots were calculated from *Xenopus* oocytes expressing $\Delta21\alpha_{1B}$ (●) and $+21\alpha_{1B}$ (○) subunits together with Ca channel β_{1b} (*A*), β_{2a} (*B*), β_3 (*C*), and β_4 (*D*) subunits. Currents were activated by brief depolarizations to various test potentials from a holding potential of −80 mV. Barium (5 mM) was the charge carrier. Normalized, averaged current traces for $\Delta21\alpha_{1B}$ (*thick line*) and $+21\alpha_{1B}$ (*thin line*) are shown superimposed as *insets* in *A–D*. Currents shown were activated by depolarization to −10 mV for β_{1b}, β_{2a}, and β_4 and, to compensate for its different voltage-dependent activation, to 0 mV for β_3. Activation midpoints for currents induced by the expression were as follows: $+21\alpha_{1B}/\beta_{1b}$, −12.7 ± 0.8 mV ($n$ = 5); $+21\alpha_{1B}/\beta_{2a}$, −12.1 ± 0.7 mV ($n$ = 6); $+21\alpha_{1B}/\beta_3$, −5.5 ± 0.7 mV (n = 5); and $+21\alpha_{1B}/\beta_4$, −13.2 ± 0.5 mV (n = 7). These values were not significantly different from $\Delta21\alpha_{1B}$ (see legend to Fig. 5 for $\Delta21\alpha_{1B}$ values).

at more depolarized voltages ($V_{1/2}$ of approximately −5 mV), current–voltage relationships were similar between β subunits (Fig. 5*A*). However, a comparison of steady-state inactivation curves highlights how similar inactivation profiles of N-type Ca channels recorded from β_{1b}- and β_4-expressing oocytes are to each other on the one hand and different from β_{2a} and β_3 on the other. This correlation could be significant in light of the fact that differences between α_{1B} splice variants are only significant when coexpressed with β_{1b} and β_4 but not β_{2a} and β_3. Figure 5*B* shows that N-type Ca channels in β_{1b}- and β_4-expressing oocytes inactivate at more hyperpolarized voltages ($V_{1/2}$ of −60 to −80 mV) relative to N-type Ca channels associated with β_{2a} and β_3, which inactivate at significantly more depolarized membrane potentials ($V_{1/2}$ of −35 to −45 mV) (Fig. 5*B*). Similar results were also obtained using 2 mM extracellular calcium rather than 5 mM barium as the permeant ion (Fig. 6).

DISCUSSION

Alternative splicing is region-specific

Alternative splicing in intracellular loop II–III of the Ca channel α_{1B} subunit mRNA is differentially regulated in distinct regions of the nervous system. Sympathetic ganglia express the highest levels of exon-containing α_{1B} mRNA (>80% of total), and in the CNS, $+21\alpha_{1B}$ mRNA levels decrease in an approximately caudal to rostral pattern, from ~50% in brainstem to <20% in neocortex. Overall, exon skipping at this splice site prevails in whole brain, consistent with the absence of the exon in α_{1B} cDNAs isolated previously from rat brain-derived cDNA libraries (Dubel

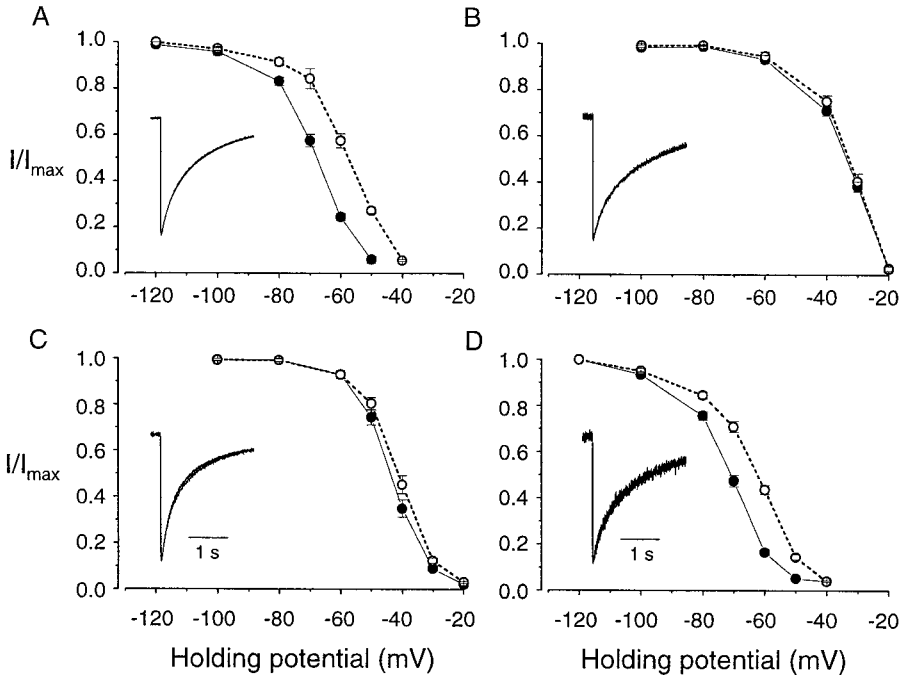

Figure 4. $+21\alpha_{1B}$ and $\Delta21\alpha_{1B}$ splice variants have different steady-state inactivation curves depending on which β subunit is coexpressed. Normalized, averaged steady-state inactivation curves were calculated from currents activated by brief depolarizations to 0 mV from various holding potentials in oocytes expressing $\Delta21\alpha_{1B}$ (●) and $+21\alpha_{1B}$ (○) subunits together with Ca channel β_{1b} (*A*), β_{2a} (*B*), β_3 (*C*), and β_4 (*D*) subunits. Normalized, averaged currents activated by long depolarizations to +20 mV are also shown for $\Delta21\alpha_{1B}$ (*thick line*) and $+21\alpha_{1B}$ (*thin line*) to compare inactivation kinetics (*insets, A–D*). Barium (5 mM) was the charge carrier. Midpoints of steady-state inactivation curves for currents induced by the expression were as follows: $+21\alpha_{1B}/\beta_{1b}$, −58.1 ± 0.8 mV ($n$ = 6); $+21\alpha_{1B}/\beta_{2a}$, −33.0 ± 0.8 mV ($n$ = 5); $+21\alpha_{1B}/\beta_3$,=−41.5 ± 0.9 mV (n = 5); and $+21\alpha_{1B}/\beta_4$, −63.3 ± 0.8 mV (n = 6). Values for $\Delta21\alpha_{1B}$ currents are in the legend to Figure 5.

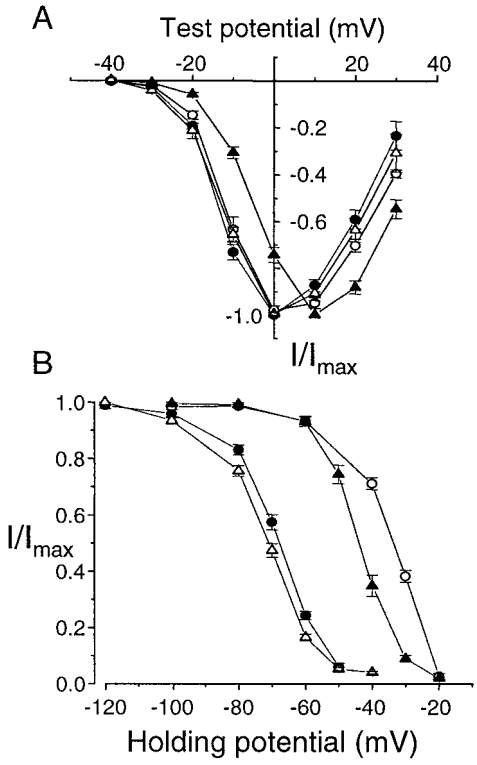

Figure 5. Functional differences in α_{1B} coexpressed with different Ca channel β subunits. N-type Ca channel currents induced by coexpressing $\Delta 21\alpha_{1B}$ with β_{1b}(●), β_{2a} (○), β_3(▲), and β_4 (△) subunits in *Xenopus* oocytes. Barium (5 mM) was the charge carrier. *A*, Currents activated by step depolarizations to various test potentials from a holding potential of −80 mV. Normalized, averaged peak current–voltage plots for each β subunit are shown. Each point is mean ± SE. Activation midpoints were as follows: $\Delta 21\alpha_{1B}/\beta_{1b}$, −13.6 ± 0.6 mV ($n$ = 6); $\Delta 21\alpha_{1B}/\beta_{2a}$, −11.7 ± 1.1 mV ($n$ = 6); $\Delta 21\alpha_{1B}/\beta_3$, −4.6 ± 1.0 mV ($n$ = 4); and $\Delta 21\alpha_{1B}/\beta_4$, −13.2 ± 0.5 mV ($n$ = 5). In the presence of β_3, currents activated at voltages ~10 mV more depolarized compared with β_{1b}, β_{2a}, and β_4. *B*, Average, steady-state inactivation curves of $\Delta 21\alpha_{1B}$ channels expressed with different β subunits. Currents were activated by depolarizations to 0 mV from different holding potentials. Peak currents were measured and expressed relative to maximum current (holding potential, −120 to −100 mV). Inactivation midpoints were as follows: $\Delta 21\alpha_{1B}/\beta_{1b}$, −68.5 ± 0.8 mV ($n$ = 6); $\Delta 21\alpha_{1B}/\beta_{2a}$, −34.1 ± 0.7 mV ($n$ = 5); $\Delta 21\alpha_{1B}/\beta_3$, −43.8 ± 1.0 mV ($n$ = 5); and $\Delta 21\alpha_{1B}/\beta_4$, −71.2 ± 0.7 mV ($n$ = 6).

et al., 1992; Fujita et al., 1993). It has been suggested recently that the II–III intracellular loop exon of α_{1B} is preferentially expressed in brain regions of the rat enriched in monoaminergic neurons, based on *in situ* hybridization and RT-PCR analysis (Ghasemzadeh et al., 1999). Our results do not test this hypothesis directly but nonetheless do favor more widespread distribution. For example, there is a relatively high representation of $+21\alpha_{1B}$ mRNA in regions of the CNS not particularly rich in monoaminergic neurons, such as spinal cord and hypothalamus (Fig. 2). The expression pattern of the II–III intracellular loop exon differs from other splice sites that we have studied previously in the IIIS3–IIIS4 and IVS3–IVS4 extracellular linkers of the α_{1B} subunit, suggesting that the α_{1B} gene contains multiple, independently regulated sites of alternative splicing.

Functional consequences of alternative splicing

The functional effect of lengthening the II–III intracellular loop of the α_{1B} subunit by 21 amino acids is summarized in Figure 6. Exon inclusion did not affect the voltage dependence of channel

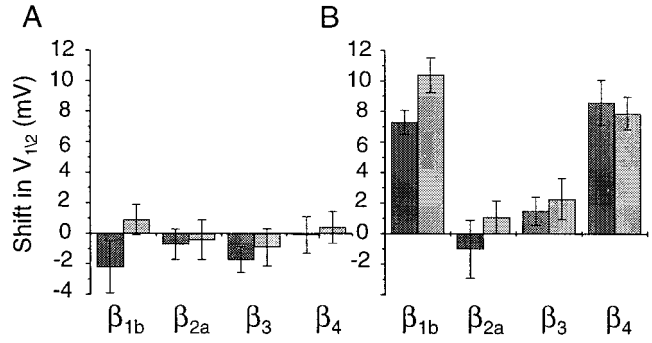

Figure 6. Functional differences between α_{1B} splice variants are β subunit-specific. Average shifts in channel activation (*A*) and steady-state inactivation (*B*) midpoints between $\Delta 21\alpha_{1B}$ and $+21\alpha_{1B}$ splice variants in the presence of different Ca channel β subunits. Currents were measured using 2 mM Ca (*dark shading*) and 5 mM Ba (*light shading*) as the permeant ions. Midpoints of activation calculated from current–voltage plots using 2 mM Ca were as follows: $\Delta 21\alpha_{1B}/\beta_{1b}$, −13.9 ± 1.2 mV ($n$ = 7); $\Delta 21\alpha_{1B}/\beta_{2a}$, −7.9 ± 0.8 mV ($n$ = 6); $\Delta 21\alpha_{1B}/\beta_3$, −5.3 ± 0.6 mV ($n$ = 4); and $\Delta 21\alpha_{1B}/\beta_4$, −14.9 ± 1.1 mV ($n$ = 5); and compared with $+21\alpha_{1B}/\beta_{1b}$, −16.1 ± 1.2 mV ($n$ = 5); $+21\alpha_{1B}/\beta_{2a}$, −8.6 ± 0.6 mV ($n$ = 6); $+21\alpha_{1B}/\beta_3$, −7.0 ± 0.6 mV (n = 5); and $+21\alpha_{1B}/\beta_4$, −15.0 ± 0.5 mV (n = 5). Midpoints from steady-state inactivation curves using 2 mM Ca as charge carrier were as follows: $\Delta 21\alpha_{1B}/\beta_{1b}$, −72.1 ± 0.6 mV ($n$ = 6); $\Delta 21\alpha_{1B}/\beta_{2a}$, −37.0 ± 1.6 mV ($n$ = 5); $\Delta 21\alpha_{1B}/\beta_3$, −41.9 ± 0.6 mV ($n$ = 5); and $\Delta 21\alpha_{1B}/\beta_4$, −72.7 ± 1.3 mV ($n$ = 7); and compared with $+21\alpha_{1B}/\beta_{1b}$, −64.4 ± 0.5 mV ($n$ = 6); $+21\alpha_{1B}/\beta_{2a}$, −38.0 ± 1.0 mV ($n$ = 5); $+21\alpha_{1B}/\beta_3$, −40.4 ± 0.7 mV (n = 5); and $+21\alpha_{1B}/\beta_4$, −64.1 ± 0.7 mV (n = 5). Values are mean ± SE. See legends to Figures 3–5 for values with 5 mM Ba as charge carrier.

activation but did induce a shift in the channel availability curve to more depolarized membrane voltages similarly with calcium or barium as permeant ion. These results contrast nicely with our analysis of alternative splicing in the IVS3–IVS4 extracellular linker of the α_{1B} subunit, a domain close to the putative voltage sensor (S4). Splicing in IVS3–IVS4 affected both the voltage dependence and kinetics of channel activation but not inactivation (Lin et al., 1997, 1999).

Functional differences between $+21\alpha_{1B}$ and $\Delta 21\alpha_{1B}$ splice variants were only observed in the presence of Ca channel β_{1b} or β_4 subunits that also shift channel steady-state inactivation curves into the physiologically interesting range of potentials between −60 and −90 mV. In contrast, small or no shifts were observed between the splice variants coexpressed with either β_{2a} or β_3 that form N channels that inactivate at significantly more depolarized voltages (−50 to −20 mV). *Xenopus* oocytes express an endogenous Ca channel β subunit that is highly homologous to mammalian β_3 (β_{3XO}) (Tareilus et al., 1997). If present at high enough levels, endogenous β_{3XO} could partially mask the actions of exogenously expressed β subunits; consequently, hyperpolarizing shifts in N-type Ca channel steady-state inactivation curves associated with β_{1b} and β_4 might be slightly underestimated. Nonetheless, our results demonstrate that functional differences between α_{1B} splice variants depend on their interactions with specific β subunits.

How does this β subunit specificity arise? One possibility is that β_{1b} and β_4 subunits, but not β_{2a} or β_3, specifically interact with the 21 amino acid insert in the II–III intracellular loop of α_{1B}. Although the primary β subunit binding site on α_1 is in the intracellular loop between domains I and II (Pragnell et al., 1993; De Waard et al., 1994), secondary β-interaction sites in the C-terminal region of α_1 have been identified recently (Walker et

al., 1998, 1999), leaving open the possibility that additional β-interaction sites in α_1, such as in the II–III loop, might exist. Alternatively, β subunit specificity might not depend on direct interactions between β subunits and the II–III intracellular loop of α_{1B}. For example, modification of N-type Ca channel inactivation might be most permissible at membrane potentials between −60 and −90 mV; consequently, differences between splice variants would surface in the presence of β_{1b} or β_4 but be less obvious with β_{2a} or β_3 subunits. In this case, functional differences between α_{1B} splice variants in native cells might also depend on interactions with other Ca channel subunits (e.g., $\alpha_2\delta$) and modulators (e.g., G-proteins) that, like β subunits, affect channel inactivation.

Our studies suggest that all α_{1B}/β combinations are permissible and form functional channels in the *Xenopus* oocyte expression system, but which combinations occur in native cells? There is significant overlap in the distribution of α_{1B} and β_3 mRNA and protein in mammalian brain but the correlation is not perfect (Ludwig et al., 1997), and biochemical studies have demonstrated significant levels of α_{1B}/β_3 and α_{1B}/β_4 complexes in native N-type Ca channel proteins isolated from brain (Scott et al., 1996). The study by Scott et al. (1996) does not, however, distinguish between different α_{1B} splice variants. Although α_{1B}, β_3, and β_4 mRNAs are broadly distributed in brain, in brainstem β_{1b} and β_4 mRNAs are present to the exclusion of β_{2a} and β_3 (Ludwig et al., 1997). Because significant levels of $\Delta21\alpha_{1B}$ and $+21\alpha_{1B}$ mRNAs (Fig. 2) are also present in brainstem, we suggest that both α_{1B} splice variants probably form native N-type Ca channels with β subunits other than β_3 (i.e., β_{1b} or β_4). In light of our results, it will now be important to establish which β subunits associate with which specific α_{1B} splice variant, $\Delta21\alpha_{1B}$ and $+21\alpha_{1B}$, in different regions of the nervous system.

The potential to mix and match multiple α_{1B} splice variants and β subunits may represent a mechanism for fine-tuning excitation–secretion coupling at different synapses. We speculate that the availability of N-type Ca channels at synapses dominated by $\Delta21\alpha_{1B}/\beta_{1b}$ or $\Delta21\alpha_{1B}/\beta_4$ complexes may be more sensitive to modulation by agents or stimuli that induce relatively prolonged changes in the resting membrane potential between −60 and −80 mV compared with β_{2a}- or β_3-dominant synapses containing either $\Delta21\alpha_{1B}$ or $+21\alpha_{1B}$. Heterogeneity in α_{1B}/β complexes (Scott et al., 1996) probably account for native N-type Ca channel currents in neurons that differ in their sensitivity to inactivation as the membrane potential is depolarized (Bean, 1989; Kongsamut et al., 1989; Plummer et al., 1989). Our results also highlight the II–III intracellular loop of the Ca channel α_{1B} subunit as a domain important for regulating N-type Ca channel availability at voltages close to the resting membrane potential. The demonstration that syntaxin, a SNARE [SNAP (soluble *N*-ethylmaleimide-sensitive factor attachment protein) receptor] that binds to a region in the II–III intracellular loop overlapping the splice junction, also affects the position of the steady-state inactivation curve is consistent with this hypothesis (Bezprozvanny et al., 1995).

Future directions

Our findings provide the framework to begin to address other questions related to the functional significance of splicing in the II–III intracellular loop of the Ca channel α_{1B} subunit. For example, the alternatively spliced exon is unusually enriched in serine and threonine residues (9 of 21), suggesting that $\Delta21\alpha_{1B}$ and $+21\alpha_{1B}$ splice variants might be differentially modulated by protein kinase. Furthermore, because the exon overlaps the synaptic protein interaction site on α_{1B} (synprint) (Catterall, 1999), it would be interesting to determine how its presence influences SNARE binding (Sheng et al., 1994; Charvin et al., 1997; Catterall, 1999). Along these lines, there is evidence for isoform-specific interactions of SNAREs with II–III intracellular loop variants of the closely related α_{1A} subunit (Rettig et al., 1996; Catterall, 1999), although the isoforms of α_{1A} reported by Catterall and colleagues do not correspond to the $\Delta21\alpha_{1B}$ and $+21\alpha_{1B}$ splice variants described here. Finally, we know very little about the mechanisms that regulate expression of this exon and other alternative spliced exons of α_{1B} in different regions of the nervous system. The identification of regulatory elements presumably in introns upstream of the exon might provide clues as to the nature of the proteins that direct these functionally significant splicing events (Grabowski, 1998).

REFERENCES

Bean BP (1989) Neurotransmitter inhibition of neuronal calcium currents by changes in channel voltage dependence. Nature 340:153–156.

Bezprozvanny I, Scheller RH, Tsien RW (1995) Functional impact of syntaxin on gating of N-type and Q-type calcium channels. Nature 378:623–626.

Bourinet E, Soong TW, Sutton K, Slaymaker S, Mathews E, Monteil A, Zamponi GW, Nargeot J, Snutch TP (1999) Splicing of alpha 1A subunit gene generates phenotypic variants of P- and Q-type calcium channels. Nat Neurosci 2:407–415.

Cahill AL, Hurley JH, Fox AP (2000) Coexpression of cloned α(1B), β(2a), and α(2)/Δ subunits produces non-inactivating calcium currents similar to those found in bovine chromaffin cells. J Neurosci 20:1685–1693.

Castellano A, Wei X, Birnbaumer L, Perez-Reys E (1993a) Cloning and expression of a third calcium channel beta subunit. J Biol Chem 268:3450–3455.

Castellano A, Wei X, Birnbaumer L, Perez-Reys E (1993b) Cloning and expression of a neuronal calcium channel beta subunit. J Biol Chem 268:12359–12366.

Catterall WA (1999) Interactions of presynaptic Ca^{2+} channels and snare proteins in neurotransmitter release. Ann NY Acad Sci 868:144–159.

Charvin N, L'Eveque C, Walker D, Berton F, Raymond C, Kataoka M, Shoji-Kasai Y, Takahashi M, De Waard M, Seagar MJ (1997) Direct interaction of the calcium sensor protein synaptotagmin I with a cytoplasmic domain of the alpha1A subunit of the P/Q-type calcium channel. EMBO J 16:4591–4596.

Coppola T, Waldmann R, Borsotto M, Heurteaux C, Romey G, Mattei M-G, Lazdunski M (1994) Molecular cloning of a murine N-type calcium channel α_1 subunit. Evidence for isoforms, brain distribution, and chromosomal localization. FEBS Lett 338:1–5.

De Waard M, Scott VE, Pragnell M, Campbell KP (1994) Ca channel beta-subunit binds to a conserved motif in I-II cytoplasmic linker of the alpha-1 subunit. Nature 368:67–70.

Dubel SJ, Starr TV, Hell JW, Ahlijanian MK, Enyeart JJ, Catterall WA, Snutch TP (1992) Molecular cloning of the α_1 subunit of an ω-conotoxin-sensitive calcium channel. Proc Natl Acad Sci USA 89:5058–5062.

Dunlap K, Luebke JI, Turner TJ (1995) Exocytotic Ca^{2+} channels in mammalian central neurons. Trends Neurosci 18:89–98.

Fujita Y, Mynlieff M, Dirksen RT, Kim MS, Niidome T, Nakai J, Friedrich T, Iwabe N, Miyata T, Furuichi T, Furuichi T, Funutama D, Mikoshiba K, Mori Y, Bean KG (1993) Primary structure and functional expression of the ω-conotoxin-sensitive N-type channel from rabbit brain. Neuron 10:585–589.

Ghasemzadeh MB, Pierce RC, Kalivas PW (1999) The monoamine neurons of the rat brain preferentially express a splice variant of alpha1B subunit of the N-type calcium channel. J Neurochem 73:1718–1723.

Goldin AL, Sumikawa K (1992) Preparation of RNA for injection into *Xenopus* oocytes. Methods Enzymol 207:279–297.

Grabowski PJ (1998) Splicing regulation in neurons: tinkering with cell-specific control. Cell 92:709–712.

Hirning LD, Fox AP, McCleskey EW, Olivera BM, Thayer SA, Miller RJ, Tsien RW (1988) Dominant role of N-type Ca^{2+} channels in evoked

release of norepinephrine from sympathetic neurons. Science 239: 57–61.

Kollmar R, Fak J, Montgomery LG, Hudspeth AJ (1997) Hair cell-specific splicing of mRNA for the alpha1D subunit of voltage-gated Ca^{2+} channels in the chicken's cochlea. Proc Natl Acad Sci USA 94:14889–14893.

Kongsamut S, Lipscombe D, Tsien RW (1989) The N-type Ca channel in frog sympathetic neurons and its role in alpha-adrenergic modulation of transmitter release. Ann NY Acad Sci 560:312–333.

Lin Z, Haus S, Edgerton J, Lipscombe D (1997) Identification of functionally distinct isoforms of the N-type Ca^{2+} channel in rat sympathetic ganglia and brain. Neuron 18:153–166.

Lin Z, Lin Y, Schorge S, Pan JQ, Beierlein M, Lipscombe D (1999) Alternative Splicing of a short cassette exon in α_{1B} generates functionally distinct N-type calcium channels in central and peripheral neurons. J Neurosci 19:5322–5331.

Ludwig A, Flockerzi V, Hofmann F (1997) Regional expression and cellular localization of the α1 and β subunit of high voltage-activated calcium channels in rat brain. J Neurosci 17:1339–1349.

Olcese R, Qin N, Schneider T, Neely A, Wei X, Stefani E, Birbaumer L (1994) The amino terminus of a calcium channel beta subunit sets rates of channel inactivation independently of the subunit's effect on activation. Neuron 13:1433–1438.

Pan J, Nam J, Lipscombe D (1999) Alternative splicing in the putative II-III loop of the N-type Ca channel α_{1B} subunit. Soc Neurosci Abstr 25:196.

Perez-Reyes E, Wei XY, Castellano A, Birnbaumer L (1990) Molecular diversity of L-type calcium channels. Evidence for alternative splicing of the transcripts of three non-allelic genes. J Biol Chem 265: 20430–20436.

Perez-Reyes E, Castellano A, Kim HS, Baggstrom E, Lacerda AE, Wei X, Birmaumer L (1992) Cloning and expression of a cardiac/brain beta subunit of the L-type calcium channel. J Biol Chem 267: 1792–1797.

Plummer MR, Logothetis DE, Hess P (1989) Elementary properties and pharmacological sensitivities of calcium channels in mammalian peripheral neurons. Neuron 2:1453–1463.

Pragnell M, Sakamoto J, Jay SD, Campbell KP (1991) Cloning and tissue-specific expression of the brain calcium channel beta-subunit. FEBS Lett 291:253–258.

Pragnell M, Sakamoto J, Jay SD, Campbell KP (1992) Cloning and tissue-specific expression of the brain calcium channel beta-subunit. J Biol Chem 267:1792–1797.

Pragnell M, De Waard M, Mori Y, Tanabe T, Snutch TP, Campbell KP (1993) Calcium channel beta-subunit binds to a conserved motif the I-II cytoplasmic linker of the alpha1-subunit. J Biol Chem 268: 12359–12366.

Rettig J, Sheng ZH, Kim DK, Hodson CD, Snutch TP, Catterall WA (1996) Isoform-specific interaction of the alpha1A subunits of brain Ca^{2+} Channel with the presynaptic proteins syntaxin and SNAP-25. Proc Natl Acad Sci USA 93:7363–7368.

Schorge S, Gupta S, Lin Z, McEnery MW, Lipscombe D (1999) Calcium channel activation stabilizes a neuronal calcium channel mRNA. Nat Neurosci 2:785–790.

Scott VE, De Waard M, Liu H, Gurnett CA, Venzke DP, Lennon VA, Campbell KP (1996) Beta subunit heterogeneity in N-type Ca^{2+} channels. J Biol Chem 271:3207–3212.

Sharp PA, Burge CB (1997) Classification of introns: U2-type or U12-type. Cell 91:875–879.

Sheng ZH, Rettig J, Takahashi M, Catterall WA (1994) Identification of a syntaxin-binding site on N-type calcium channels. Neuron 13:1303–1313.

Soldatov NM (1994) Genomic structure of human L-type Ca^{2+} channel. Genomics 22:77–87.

Takahashi T, Momiyama A (1993) Different types of calcium channels mediate central synaptic transmission. Nature 366:156–158.

Tareilus E, Roux M, Qin N, Olcese R, Zhou J, Stefani E, Birnbaumer L (1997) A *Xenopus* oocyte beta subunit: evidence for a role in the assembly/expression of voltage-gated calcium channels that is separate from its role as a regulatory subunit. Proc Natl Acad Sci USA 94:1703–1708.

Walker D, De Waard M (1998) Subunit interaction sites in voltage-dependent Ca^{2+} channels: role in channel function. Trends Neurosci 21:148–154.

Walker D, Bichet D, Campbell KP, De Waard M (1998) A beta 4 isoform-specific interaction site in the carboxyl-terminal region of the voltage-dependent Ca^{2+} channel alpha 1A subunit. J Biol Chem 273:2361–2367.

Walker D, Bichet D, Geib S, Mori E, Cornet V, Snutch TP, Mori Y, De Waard M (1999) A new beta subtype-specific interaction in alpha1A subunit controls P/Q-type Ca^{2+} channel activation. J Biol Chem 274: 12383–12390.